LONGITUDINAL—TRANSVERSE LIQUID FILTRATION IN AN ANNULAR HEAT-LIBERATING MEDIUM

A. P. Akhramovich, V. P. Kolos,
and V. N. Sorokin

UDC 621.039.517.5:532.546

Breakaway flow zones close to the ends of a layer in longitudinal—transverse liquid filtration are experimentally observed. In a linear approximation, the problem of determining the form of the ends of the layer for which there is no flow breakaway is solved.

The clearly expressed potential benefits of equipment with operating elements which include annular heat-liberating layers with lateral liquid supply indicate the appearance of a qualitatively new, promising trend in the development of reactor construction; such equipment may be successfully used in the chemical industry, the power industry, and thermal engineering [1-7].

A line diagram of the working element is shown in Fig. 1: liquid from the receiver is fed to the distributive channel; moving along this channel, it is filtered in the radial direction through a dense layer, takes up the heat generated there, and leaves the system through the output channel.

The completeness with which all the advantages of the radial-type heat-liberating equipment may be used, the means involved in their development, and their rate of introduction depend directly on the adequacy of mathematical modeling of the fluid motion in the working element. The methods developed for calculating the thermohydrodynamic parameters of the flow in this apparatus and the choice its optimal size are based on one-dimensional models of the fluid motion in the layer [6, 8, 9]. Their clarity and mathematical simplicity play a positive role in establishing the expediency of developing radial heat-generating equipment. However, the internal contradiction of this model — the simultaneous existence of an axial component of the pressure gradient in the layer and strictly radial motion of the fluid — indicates that theoretical work on the development of reliable calculation methods is incomplete.

This contradiction appears again, though in somewhat different form, in the analysis of two-dimensional fluid filtration close to the ends of the layer. In fact, the pressure drop with fluid motion in the channels of the working element, in particular at the input and output, leads to the appearance of an axial component of the pressure gradient at the ends of the layer; if the classical Darcy model is taken as the basic law of filtration, the presence of an axial component of the pressure gradient at the ends of the layer is inconsistent with their impermeability. Taking account of inertial (quasi-ideal-fluid model [10, 11]) or viscous [12, 13] forces eliminates this inconsistency, but it is often found that the thickness of "boundary layer" at the ends of the working element is comparable with the size of the fraction. Thus, close to the ends of the layer, the fluid motion does not always conform to the known law of filtration.

In a complicated situation, visual observation of the fluid flow pattern is undertaken. A plane model of a working element with organic-glass walls is prepared. The layer of dimensions 400 × 70 × 40 mm is assembled from the glass spheres of diameter 3 mm. The construction of the model allows the angle of slope α and the gap between the channel walls and the lattices enclosing the layer δ to be varied within the limits α = 0-0.122 rad, δ = 0-50 mm. Water is fed to the receiver from a controllable bypass valve by means of two KMV8-18 pumps connected in parallel, and then goes to the distributive channel and further along the system. The whole water flux is periodically colored prior to entry in the distributive channel.

Institute of Nuclear Power, Academy of Sciences of the Belorussian SSR, Minsk. Translated from Inzhenerno-Fizicheskii Zhurnal, Vol. 52, No. 5, pp. 756-765, May, 1987. Original article submitted February 26, 1986.

0022-0841/87/5205-0547$12.50

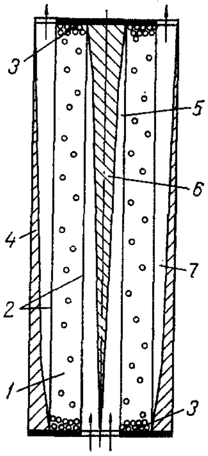

Fig. 1. Line diagram of working element with plane ends: 1) annular heat-liberating unit; 2) enclosing lattice; 3) end surfaces; 4) casing; 5) distributive channel; 6) displacing rod; 7) output channel.

It may be established that, after switching off the dye supply, the basic part of the flow becomes transparent almost instantaneously; at the same time, dark (dyed) regions remain close to the ends of the layer (Fig. 2). They must be regarded as zones of breakaway flow. Approximately 12-14 sec after the end of dying, the dark spots are resorbed.

The relatively low level of exchange between the fluid in the breakaway zone and the basic flow limits the rate of heat transfer in power equipment or has a negative influence on the quality of the production obtained in chemical equipment. Eliminating these negative hydrodynamic effects in the heat-liberating layer at the given moment is the basic problem. A solution of the conjugate problem of determining the thermohydrodynamic parameters of the flow and the form of the end surfaces of the layer for which there is no breakaway zone is outlined below.

Consider steady axisymmetric fluid motion in a working element. For its description, a cylindrical coordinate system is introduced, with its z axis along the axis of construction in the direction of fluid motion; its origin is in the plane of the input to the distributive channel.

In the mathematical modeling, the molecular heat transfer, radiant energy transfer, gravity, and heating of the liquid as a result of dissipation are excluded from consideration [11, 14]. The energy liberation in particles of the layer are modeled by internal heat sources concentrated in the fluid.

The inertial forces in filtration are basically concentrated in a narrow space at the liquid input and output for the layer; therefore, its motion outside the breakaway zones is described by the equations

$$\nabla P = -k\rho|\mathbf{V}|\mathbf{V};\ k = \frac{1{,}7(1-\varepsilon)}{\varepsilon^3 d}; \tag{1}$$

$$\rho\mathbf{V}\cdot\nabla I = q; \tag{2}$$

$$\nabla\rho\mathbf{V} = 0, \tag{3}$$

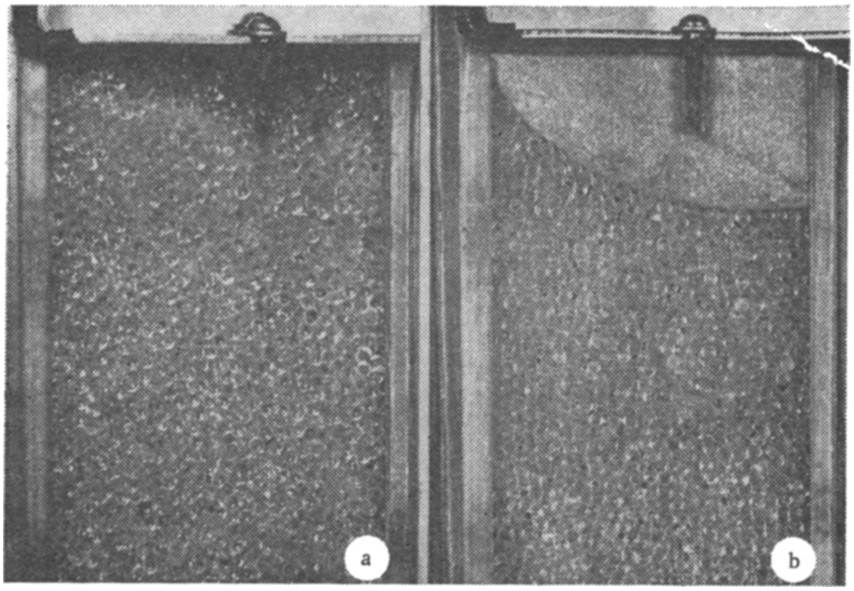

Fig. 2. Photographs of the fluid flow patterns in the front section of the layer in a model of the working element (side view): a) with plane and surfaces orthogonal to the axis of construction (the dark region close to the end is a breakaway-flow zone): b) with shaped ends (no breakaway flow).

and the influence of inertial effects on the behavior of the flow is taken into account by matching conditions at the interface between the channel medium and the dense layer

$$[P]=0;\ [I]=0;\ [V_x]=0;\ \frac{dG_{1,2}}{dx}=\mp 2\pi (R\rho V_r)^*_{1,2}; \tag{4}$$

in writing Eq. (4), the pressure and enthalpy discontinuity at the interface is neglected [15], since the corresponding contribution to the total drop in these quantities between the distributive and output channels is small.

The fluid motion in the channels themselves is described by means of one-dimensional equations [6, 16]

$$\left(\rho\frac{dP}{dx}\right)_{1,2}=\left(-\frac{3}{2}\frac{G}{F^2}\frac{dG}{dx}+\frac{G^2}{F^3}\frac{dF}{dx}+\frac{G^2}{F^2\rho}\frac{d\rho}{dx}-\frac{\xi G^2}{2F^2D}\right)_{1,2}; \tag{5}$$

$$I_1=I_1^*=I_0; \tag{6}$$

$$I_2=G_2^{-1}\int\limits_{\Delta}^{x} I_2^*\frac{dG_2}{dx}dx; \tag{7}$$

$$\lg\xi_{1,2}=-1{,}41-0{,}097\log_2(D/60m)_{1,2}; \tag{8}$$

the heat-carrier density is calculated in the Boussinesq approximation

$$\rho=\frac{c}{I}. \tag{9}$$

The relation between the filtrations Eqs. (1)-(3) and Eqs. (5)-(8) is established by means of the condition of dynamic matching at the channel—layer boundary

$$\frac{dP_{1,2}}{dx}=\frac{\partial P}{\partial x}(x;\ R_{1,2}), \tag{10}$$

which, strictly speaking, only holds approximately.

The known quantities in modeling are taken to be: fluid pressure at the input to the working element P_0; the incoming fluid flow rate G_0; the grain diameter d; the length of the redistributive channel L, the radii of the layer lateral surfaces $R_{1,2}$; the volume energy liberation q(x, r); the liquid enthalpy at the input to the working element I_0; the relative roughness of the channel walls $(m/D)_{1,2}$; the cross sections of the channels $F_1(x)$ and $F_2(x^0)$ and their derivatives dF_1/dx, dF_2/dx^0. The longitudinal coordinates x and x^0 are related by the translation relation

$$x^0 = x - \Delta. \tag{11}$$

It follows from the definition of the streamline that nonbreakaway fluid flow in the layer entails coincidence between the end surfaces and the surfaces formed by the streamlines at the edges of the layer for a flow conforming to the filtration law in Eqs. (1)-(3); hence, the desired form of the layer ends must be determined by integrating the equation

$$\frac{dx}{dr} = \frac{V_x}{V_r} = \frac{\partial P}{\partial x} \Bigg/ \frac{\partial P}{\partial r}; \quad x|_{r=R_1} = (0 \wedge L). \tag{12}$$

The solution of Eq. (12) with the boundary conditions $x|_{r=R_1} = x^*$ is written as a power series, retaining only the first three terms

$$x = x^* + a(x^*)(r - R_1) + \frac{b(x^*)}{(R_2 - R_1)}(r - R_1)^2. \tag{13}$$

This problem reduces to determining the dimensionless functions a, b.

The mathematical computations are conducted to second order of smallness with respect to a, b; the final system of equations is reduced to the form $y_i' = f_i(x, y_1, \ldots, y_n)$ convenient for computer solution.

After substituting Eq. (13) into the streamline equation, the relation between the components of the velocity vector in the layer is established

$$V_x = V_r\left[a + \frac{2b(r - R_1)}{(R_2 - R_1)}\right], \tag{14}$$

which allows Eqs. (2) and (3) to be brought to quasilinear form.

In this case, the continuity equation takes the form

$$\frac{\partial \rho r V_r}{\partial r} + \frac{\partial \rho r V_r}{\partial x}\left(a + 2b\frac{r - R_1}{R_2 - R_1}\right) = -r\rho V_r\left[a' + \frac{2b'}{R_2 - R_1}(r - R_1)\right];$$

$$r\rho V_r|_{r=R_1} = -\frac{1}{2\pi}\frac{dG_1}{dx};$$

approximate solution leads to the result

$$2\pi r\rho V_r = -\frac{dG_1}{dx}\exp - \int_{R_1}^{r}\left\{a' + \frac{2b'}{(R_2 - R_1)}(r - R_1) + \left[a'' + \frac{2b''}{R_2 - R_1}(r - R_1)\right]\left[a(r - R_1) + \frac{b}{R_2 - R_1}(r - R_1)^2\right]\right\}dr. \tag{15}$$

Here and below, a prime denotes derivatives with respect to x.

Linearizing Eq. (15) considerably simplifies the mathematical description of the velocity field

$$2\pi r\rho V_r = -\frac{dG_1}{dx}\left[1 - a'(r - R_1) - \frac{b'}{R_2 - R_1}(r - R_1)^2\right]. \tag{16}$$

The approximate solution of the energy equation

$$\frac{\partial I}{\partial r}+\frac{\partial I}{\partial x}\left(a+2b\,\frac{r-R_1}{R_2-R_1}\right)=\frac{2\pi rq}{\frac{dG_1}{dx}\left[1-a'(r-R_1)-\frac{b'}{R_2-R_1}(r-R_1)^2\right]},$$

$$I|_{r=R_1}=I_0,$$

allows the thermal field of the flow inside the layer to be estimated

$$I=I_0-2\pi\left(\frac{dG_1}{dx}\right)^{-1}\int\limits_{R_1}^{r} r\left\{q+\frac{\partial q}{\partial x}\left[a(r-R_1)+\frac{b}{R_2-R_1}(r-R_1)^2\right]\right\}dr. \tag{17}$$

Projecting Eq. (1) onto the R axis, substituting Eqs. (9), (14), (16), and (17) into the result obtained, and then integrating over the interval $[R_1;\ R_2]$, the difference between the pressures in the distributive and output channels when $V_r > 0$ is determined

$$P_1-P_2=-\frac{dG_1}{dx}\left(A^+-A\,\frac{dG_1}{dx}\right)+a'\,\frac{dG_1}{dx}\left(B^+-B\,\frac{dG_1}{dx}\right)+b'\,\frac{dG_1}{dx}\left(C^+-C\,\frac{dG_1}{dx}\right)-\frac{dG_1}{dx}(aB^-+bC^-). \tag{18}$$

The following notation is employed here

$$B^-=\frac{k}{2\pi c}\int\limits_{R_1}^{R_2}\frac{1}{r^2}\int\limits_{R_1}^{r} z(z-R_1)\frac{\partial q}{\partial x}dzdr;$$

$$C^-=\frac{k}{2\pi c(R_2-R_1)}\int\limits_{R_1}^{R_2}\frac{1}{r^2}\int\limits_{R_1}^{r} z(z-R_1)^2\frac{\partial q}{\partial x}\,dzdr;$$

$$A^+=\frac{k}{2\pi c}\int\limits_{R_1}^{R_2}\frac{1}{r^2}\int\limits_{R_1}^{r} zqdzdr;\qquad B^+=\frac{k}{\pi c}\int\limits_{R_1}^{R_2}\frac{r-R_1}{r^2}\int\limits_{R_1}^{r} zqdzdr;$$

$$C^+=\frac{k}{\pi c(R_2-R_1)}\int\limits_{R_1}^{R_2}\frac{(r-R_1)^2}{r^2}\int\limits_{R_1}^{r} zqdzdr;\qquad A=\frac{k(R_2-R_1)}{4\pi^2\rho_0 R_1R_2};$$

$$B=\frac{k}{2\pi^2\rho_0}\left(\ln\frac{R_2}{R_1}-\frac{R_2-R_1}{R_2}\right);\qquad C=\frac{k}{2\pi^2\rho_0}\left(1-\frac{2R_1}{R_2-R_1}\ln\frac{R_2}{R_1}+\frac{R_1}{R_2}\right).$$

Using Eqs. (4) and (10) and the filtration law in the form in Eq. (1), the derivatives are determined

$$\frac{dP_1}{dx}=\frac{ka}{(2\pi R_1)^2\rho_0}\left|\frac{dG_1}{dx}\right|\frac{dG_1}{dx}; \tag{19}$$

$$\frac{dP_2}{dx}=-\frac{k(a+2b)}{(2\pi R_2)^2c}\,I_2^*\left|\frac{dG_2}{dx}\right|\frac{dG_2}{dx}. \tag{20}$$

Substituting Eq. (19) into Eq. (5), the kinematic equation of the flow in the distributive channel is obtained; it is used to establish the dependence of the direction of filtration on the form of the distributive channel

$$\operatorname{sign}\left(\frac{dG_1}{dx}\right)=\operatorname{sign}\left(\frac{1}{F_1}\frac{dF_1}{dx}-\frac{\xi_1}{2D_1}\right). \tag{21}$$

It follows from Eq. (21) that the working elements whose distributive channels have a cross section described by monotonically decreasing functions are the most effective. For such devices, the derivative of the flow rate is found from the kinematic equation of the fluid flow in the distributive channel

$$\frac{dG_1}{dx}=\frac{2(\pi R)^2G}{kaF}\left[\frac{3}{2F}-\sqrt{\frac{9}{4F^2}+\frac{ka}{(\pi R)^2}\left(\frac{\xi}{2D}-\frac{1}{F}\frac{dF}{dx}\right)}\right]\Bigg|_1\overset{\text{def}}{=}M_1. \tag{22}$$

The new variable

$$U=I_2G_2 \tag{23}$$

is introduced; hence, in accordance with Eqs. (7), (9), and (23)

$$\rho_2=\frac{cG_2}{U};\qquad \frac{d\rho_2}{dx}=\frac{c}{U}\left(1-\frac{G_2}{U}I_2^*\right)\frac{dG_2}{dx}, \tag{24}$$

where

$$I_2^*=I_0-\frac{2\pi}{M_1}\int\limits_{R_1}^{R_2}r\left\{q+\frac{\partial q}{\partial x}\left[a(r-R_1)+\frac{b}{R_2-R_1}(r-R_1)^2\right]\right\}dr. \tag{25}$$

Substituting Eqs. (20) and (24) into Eq. (5) gives the kinematic equation of the flow in the output channel

$$\frac{k(a+b)}{(2\pi R)^2c}I^*\left|\frac{dG}{dx}\right|\frac{dG}{dx}-\frac{U}{cF^2}\left(\frac{1}{2}+\frac{cI^*}{U}\right)\frac{dG}{dx}+\frac{GU}{F^2c}\left(\frac{1}{F}\frac{dF}{dx}-\frac{\xi}{2D}\right)\Bigg|_2=0; \tag{26}$$

analysis of this equation, together with Eqs. (7), (17), and (23) shows that when

$$\min\left(\frac{\xi}{2D}-\frac{1}{F}\frac{dF}{dx}\right)_2>0 \tag{27}$$

fluid injection into the output channel occurs over the whole length of the working element, i.e., $dG_2/dx > 0$.

Solving Eq. (26) for G_2', under the assumption that the constraint in Eq. (27) holds, it is found that

$$\frac{dG_2}{dx}=\frac{2(\pi R)^2}{k(a+b)I^*}\left[\frac{U}{F^2}\left(\frac{1}{2}+\frac{GI^*}{U}\right)+\sqrt{\left[\frac{U}{F^2}\left(\frac{1}{2}+\frac{GI^*}{U}\right)\right]^2-\frac{k(a+b)I^*GU}{(\pi RF)^2}\left(\frac{1}{F}\frac{dF}{dx}-\frac{\xi}{2D}\right)}\right]\Bigg|_2\overset{\text{def}}{=}M_2, \tag{28}$$

where, in view of Eqs. (11) and (13)

$$F_2=F_2(x-\Delta);\qquad \frac{dF_2}{dx}=\frac{dF_2}{dx^0}(x-\Delta);\qquad \Delta=(a(0)+b(0))(R_2-R_1).$$

The differential equation

$$\frac{dU}{dx}=I_2^*M_2, \tag{29}$$

determining the thermal power of the flux in the output channel, is easily found from Eqs. (7) and (23).

Setting $r = R_2$ in Eq. (16) and then matching the result with Eqs. (4), (22), and (28), the relation between the fluid flow rates in the channels is found: $M_2=-M_1[1-(R_2-R_1)(a'+b')]$. This equation, together with Eq. (18), is solved for a', b'

$$\frac{da}{dx}=\frac{A^+-AM_1+aB^-+bC^-+\dfrac{P_1-P_2}{M_1}-\dfrac{M_1+M_2}{M_1(R_2-R_1)}(C^+-CM_1)}{B^+-C^+-M_1(B-C)}; \tag{30}$$

$$\frac{db}{dx}=\frac{\frac{M_1+M_2}{M_1(R_2-R_1)}(B^+-BM_1)+\frac{P_1-P_2}{M_1}+A^+-AM_1-aB^--bC^-}{B^+-C^+-M_1(B-C)}.$$

In the light of Eqs. (22) and (28), Eqs. (19) and (20) describing the pressure drop in the channels take on the form

$$\frac{dP_1}{dx}=-\frac{ka}{(2\pi R_1)^2\rho_0}M_1^2;\quad \frac{dP_2}{dx}=-\frac{k(a+2b)}{(2\pi R_2)^2c}I_2^*M_2^2. \tag{31}$$

Completing the solution of the problem, the boundary conditions are now formulated. At the end of the distributive channel and the beginning of the output channel, the fluid flow rate must be zero

$$G_1|_{x=L}=0;\qquad G_2|_{x=\Delta}=0; \tag{32}$$

the continuity property of the fluid, in turn, leads to the conditions

$$G_1|_{x=0}=G_2|_{x=L+(a(L)+b(L))(R_2-R_1)}=G_0. \tag{33}$$

Although Eqs. (22) and (28) are of first order, they may satisfy the boundary conditions in Eqs. (32) and (33) since they include elements of the arbitrariness in the form of the functions a, b. In solving the problem, it is expedient to specify boundary conditions of the type

$$a|_{x=0}=a_0;\qquad b|_{x=0}=b_0$$

and in the course of computer calculation the values of a_0, b_0 are varied so as to satisfy Eqs. (32) and (33) at the end of the working element; in this formulation, the boundary conditions are explicitly determined and fixed in space. On the basis of Eqs. (23) and (32), it is found that

$$U|_{x=\Delta}=0. \tag{34}$$

It follows from the conditions of the problem that

$$P_1|_{x=0}=P_0. \tag{35}$$

Integration of Eq. (1) along the streamline leads to the result

$$P_2|_{x=\Delta}=P_0-\frac{kM_1^2(0)}{(2\pi)^2\rho_0}\frac{R_2-R_1}{R_1R_2}+\frac{kM_1(0)}{2\pi c}\int\limits_{R_1}^{R_2}\frac{1}{r^2}\int\limits_{R_1}^{r}z\tilde{q}dzdr, \tag{36}$$

where

$$\tilde{q}=q\left(a(0)(z-R_1)+\frac{b(0)}{R_2-R_1}(z-R_1)^2;\ z\right).$$

The system in Eqs. (22) and (28)-(31) with the boundary conditions in Eqs. (32)-(36), complemented by Eqs. (8) and (25), describes the thermodynamics of the working element and the form of its ends ensuring nonbreakaway longitudinal—transverse filtration in the layer.

As an illustration, the working element of a heat-generating equipment cooled by nitrogen tetroxide is calculated. The initial data are: T_0 = 453°K; P_0 = 17.5 MPa; G_0 = 12.5 kg/sec; R_1 = 0.09 m; R_2 = 0.35 m; F_1 = $0.0176[(L-x)/L]$ m^2; F_2 = $0.0808(x^0/L)$ m^2; d = $2\cdot10^{-3}$ m; q = $1.55\ [1/\pi-[(\pi-1)/2]\sin\pi(x/L)][(3R_2-r)/1.6(R_2-R_1)]\cdot10^6$ kW/m^3; $(m/D)_{1,2}$ = 0.0357; the coolant properties may be found in [17]. The cross sections of the channels are deliberately specified so that the fluid filtration does not correspond to optimal heat transfer in the layer; this allows the operation of the mathematical model here developed to be more completely demonstrated. The basic results of the calculations are shown in Fig. 3.

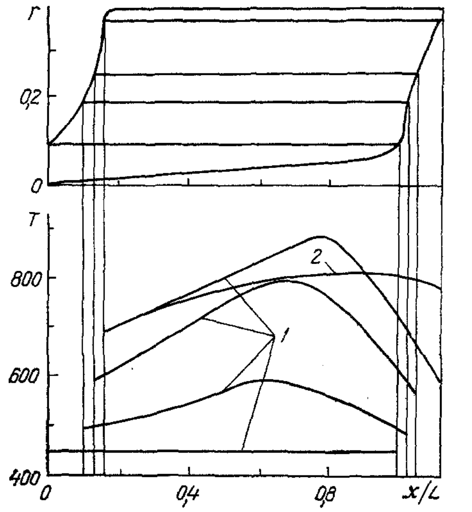

Fig. 3. Contour of working element with end surfaces ensuring nonbreakaway fluid motion and the temperature field of the flow: 1) in the heat-liberating layer; 2) in the breakaway channel.

Experimental verification indicates high recommendation of the mathematical model (Fig. 2); it must be used for initial engineering analysis of heat-generating equipment of radial type.

NOTATION

μ, P, I, ρ, dynamic viscosity, static pressure, enthalpy, and density of the liquid; V, flow-velocity vector in layer; q, volume energy liberation in the layer; d, grain diameter; ε, porosity of layer; R, radius of lateral surface of layer; L, length of distribution channel; G, fluid flow rate in channel; F, D, m, ξ, cross section, equivalent hydraulic diameter, height of roughness element of walls, and hydraulic drag of channel, respectively; U, thermal power of flow in breakaway channel; Δ, z coordinate of the line of intersection of the front end wall with the external lateral surface of the layer; r, (z), x, current cylindrical coordinates; an asterisk denotes quantities at the lateral surface of the layer. Indices: 1, distributive channel; 2, output channel; 0, input to working element; 1, 2 denotes relations which are valid for both the distributive and output channels.

LITERATURE CITED

1. S. P. Sergeev and V. V. Dil'man, Khim. Prom., No. 8, 469-470 (1982).
2. G. Perona, Energ. Nucl., 11, No. 2, 92-100 (1964).
3. H. Barthels, "Wärme- und strömungstechnische Untersuchungen zur Verwendung von directgekühlten Coated-Particle-Schüttungen in Brennelementan," Ber. Kernforsh. Jul., No. 824 (1972).
4. Dzh. Ieliovlis, At. Tekh. Rub., No. 3, 14-21 (1973).
5. A. I. Khoperskii, At. Tekh. Rub., No. 10, 3-13 (1970).
6. V. P. Kolos, V. N. Sorokin, and S. M. Kochemazov, Organization of Rational Gas Motion in Heat-Generating Pile of Hopper Type. Preprint No. 5 [in Russian], Institute of Nuclear Power, Academy of Sciences of the Belorussian SSR, Minsk (1984).
7. E. P. Sheludyakov and I. E. Chernyakov, Improving the Technology and Organizing the Sampling and Postsampling Treatment of Grains [in Russian], Novosibirsk (1983), pp. 135-142.
8. L. L. Kalishevskii, V. G. Krapivtsev, O. I. Shanin, and R. R. Khazeev, Tr. MVTU, No. 307, part 4, 73-97 (1979).
9. V. V. Dil'man, S. P. Sergeev, and V. S. Genkin, Teor. Osn. Khim. Tekhnol., 5, No. 4, 564-572 (1971).
10. A. M. Vaisman and M. A. Gol'dshtik, Izv. Akad. Nauk SSSR, Mekh. Zhidk. Gaza, No. 6, 89-95 (1978).
11. M. A. Gol'dshtik, Transfer Processes in a Granular Layer [in Russian], Novosibirsk (1984).
12. M. D. Segal' and L. P. Smirnov, Formulation of the Problem of Calculating the Velocity, Temperature, and Pressure Fields in the Hydraulic Channel of a Reactor. Preprint No. 2924 [in Russian], I. V. Kurchatov Institute of Atomic Power, Moscow (1977).

13. L. P. Smirnov and M. D. Segal', Mathematical Model for Calculating the Velocity, Temperature, and Pressure Fields in a Hydraulic Channel with a "Porous" Energy-Liberating Medium. Preprint No. 3049 [in Russian], I. V. Kurchatov Institute of Atomic Power, Moscow (1978).
14. H.-J. Lin and S. Horvath, Chem. Eng. Sci., 36, No. 1, 47-55 (1981).
15. V. P. Kolos and V. N. Sorokin, Dokl. Akad. Nauk BSSR, 28, No. 8, 713-716 (1984).
16. V. P. Kolos and V. N. Sorokin, Dokl. Akad. Nauk BSSR, 25. No. 6, 526-529 (1981).
17. V. B. Nesterenko (ed.), Physicochemical and Thermophysical Properties of the Chemically Reacting System $N_2O_4 \rightleftharpoons 2NO_2 \rightleftharpoons 2NO + O_2$ [in Russian], Minsk (1976).

MOTION OF GAS–LIQUID SYSTEMS, TAKING ACCOUNT OF MICRONUCLEUS FORMATION

R. M. Sattarov and P. Ya. Farzane

UDC 532.529.5

A model is proposed for the motion of a gas–liquid system in tubes. The theoretical and experimental results are in good agreement.

The complexity and multiplicity of the flow systems leads to considerable difficulties in studying the motion of gas–liquid systems in tubes, both in conducting the experiments and in constructing the mathematical models. Nevertheless, there have already been many experimental and theoretical investigations of the motion of gas–liquid flows in tubes (see [1-5], etc.), in which processes at pressures below the saturation pressure are mainly considered.

However, gas–liquid flows at pressures above or close to the saturation pressure are investigated as homogeneous systems, as a rule, on the assumption that transitions from one state to another occur instantaneously in the equilibrium thermodynamic theory of phase transitions.

However, according to the data of [6], the formation of a new phase occurs not instantaneously over the whole volume but rather takes the form of local fluctuations passing beyond the limits of a single aggregate state. Nuclei of new phase (gas bubbles) are "heterophase" and it is assumed, in accordance with the results of [6], that in the region above and especially close to the saturation pressure the system is not completely homogeneous. The "heterophase" system may be both in equilibrium and in a nonequilibrium state. As a rule, in the given conditions, the dispersed gas is uniformly distributed over the liquid volume.

Experiment shows [7, 8] that in a point volume the pressure level and its rate of change influence the formation of micronuclei. In connection with this, experiments are conducted to determine the moment of appearance of micronuclei of the gas phase. In a container connected to a press, a gasified liquid is prepared; it consists of transformer oil and carbon dioxide at the saturation pressure (0.04 MPa). Then the pressure is increased systematically to 0.25 MPa, i.e., considerably above the saturation pressure. Then the pressure drops systematically reduced at a definite rate to different levels above the saturation pressure. Analysis of the experimental results shows that, beginning at some value ($P = 0.17$ MPa), the pressure increases over time. As the pressure approaches the saturation level, it increases more rapidly (Fig. 1); this may be due to the formation of micronuclei of gas phase.

The presence of micronuclei in the system leads to a significant dependence of the density on the pressure and the rate of change in pressure, and probably is responsible for the decrease in values of the rheological parameters observed experimentally in [9, 10].

Taking account of the foregoing, a model may be proposed for the motion of gas–liquid systems in tubes at pressures above or close to the saturation pressure.

1. The system of differential equations for the motion of the gas–liquid medium is written as in [11]

M. Azizbekov Azerbaidzhan Institute of Petroleum and Chemistry, Baku. Translated from Inzhenerno-Fizicheskii Zhurnal, Vol. 52, No. 5, pp. 765-772, May, 1987. Original article submitted January 6, 1986.

0022-0841/87/5205-0555$12.50